Hindawi
International Journal of Aerospace Engineering
Volume 2019, Article ID 2650842, 9 pages
https://doi.org/10.1155/2019/2650842

Research Article

Aeroacoustic Investigation of Passive and Active Control on Cavity Flowfields Using Delayed Detached Eddy Simulation

Yu Liu,[1] **Yong Shi**,[1,2] **Mingbo Tong**,[2] **Fei Zhao**,[1] **and Binqi Chen**[3]

[1]*Institute of Manned Space System Engineering, Beijing 100094, China*
[2]*College of Aerospace and Engineering, Nanjing University of Aeronautics and Astronautics, Nanjing 210016, China*
[3]*School of Aeronautics and Astronautics, University of Electronic Science and Technology of China, Chengdu 611731, China*

Correspondence should be addressed to Yu Liu; yuliunuaa@163.com

Received 24 March 2019; Revised 21 August 2019; Accepted 30 August 2019; Published 21 October 2019

Academic Editor: Gustaaf B. Jacobs

In the present study, CFD simulation with delayed detached eddy simulation (DDES) is performed to investigate an open cavity at Mach 0.85. A clean cavity and cavity with passive and active control methods, including sawtooth spoiler, flat-top spoiler, crossflow rod, and steady leading edge blowing, are analyzed. The results obtained from all the control methods are compared with clean cavity, and all the flow control methods show positive effect on the overall sound pressure level reduction with the decrement up to 8 dB. The effect of active control on sound pressure level in the cavity is much better than that of passive control, with the magnitude of tone noise decreasing by 20-30 dB. The main focus of this investigation is to test the noise suppression effect by passive and active control methods.

1. Introduction

Combat aircraft such as J-20 and F-22 are now facing a big challenge, which is an aeroacoustic resonance phenomenon occurring on a weapon bay [1]. The weapon bay as shown in Figure 1 is an open cavity structure and usually has a length-to-depth ratio of 4~6. The flowfields inside the cavity present an intense unsteady process with tens of thousands of vortexes impacting with each other causing an energy exchange. The resonance arises from the cavity which leads aeroacoustic noise generated from the cavity with the level up to 170 dB. The tone noise potentially causes structural damage and failure of electronic equipment.

The research on cavity aeroacoustic mainly focuses on the mechanism of a cavity with different configurations and control effectiveness including active and passive methods. Some research into the mechanism of cavity flow and methods to improve the cavity environment has been undertaken. Zhang et al. [2] carried out wind tunnel tests and CFD analysis on cavities with different sizes. Chung [3] studied the cavity flow under different Mach numbers. The passive control methods involve manipulating the cavity geometry by adding external devices to deliberately alter the flow inside the cavity. Shaw [4] conducted a full-scale fly test on the cavity of F-111 under Mach number from 0.7 to 1.4 with three kinds of passive control methods verified. Liu and Tong [5] performed simulation on a clean cavity to investigate the effect of two kinds of spoilers at the leading edge of the cavity. The second type, known as active flow control, involves altering the flow within the cavity through the addition of devices that require external energy input. Schmit and Raman [6] compared the effectiveness of zero-low- and high-frequency flow control methodologies when applied to a generic weapon bay cavity. Yang et al. [7] investigated the suppression effect of zero-net-mass-flux jet on aerodynamic noise inside open cavities.

In this paper, three kinds of passive control devices, sawtooth spoiler, flat-top spoiler, and crossflow rod, were simulated using delayed detached eddy simulation. The active flow control methods which were steady leading edge blowing with two blowing rates were also studied to investigate the aeroacoustic noise inside the cavity.

Figure 1: Weapon bay on J-20.

2. DDES

The aerodynamic noise problem is caused by the impact of a multiscale vortex inside the cavity in essence. It is particularly critical to accurately simulate the vortex structure, especially the vortex near the shear layer. Because of time-averaged treatment of the flowfields, the Reynolds-averaged Navier-Stokes method (RANS) cannot simulate the vortex structures of all scales so it is impossible to accurately predict the sound pressure level inside the cavity. Although the vortex structures of various scales in the cavity can be well simulated by large eddy simulation (LES), the research of Li. et al. [8] shows that the cost of LES in the region of the boundary layer or shear layer is too high under the condition of the high Reynolds number. This research followed the methods of Liu and Tong [9] in 2014. Detached eddy simulation (DES) as a hybrid of RANS and LES [10] has high prediction accuracy for large-scale separation while having low requirements for computation cost. In the previous study [9], the DES method was verified on a clean cavity and the accuracy was acceptable by comparing with the experiment.

The one-equation Spalart-Allmaras (S-A) model can be written as

$$\frac{\partial \tilde{\nu}}{\partial t} + u_i \frac{\partial \tilde{\nu}}{\partial x_i} = \frac{1}{\sigma}\left[\nabla\cdot((\nu+\tilde{\nu})\nabla\tilde{\nu}) + C_{b2}(\nabla\tilde{\nu})^2\right] + P(\tilde{\nu}) - D(\tilde{\nu}), \tag{1}$$

where the dissipation is defined as

$$D(\tilde{\nu}) = C_{w1} f_w \left(\frac{\tilde{\nu}}{d}\right)^2, \tag{2}$$

and the production term

$$P(\tilde{\nu}) = C_{b1}\tilde{\nu}\tilde{\Omega}, \tag{3}$$

where $\tilde{\nu}$ is the turbulence variable and ν is the kinematic viscosity. σ, C_{b1}, C_{b2}, and κ are constants. The vorticity variable is given by $\tilde{\Omega} = |\Omega| + (\tilde{\nu}/\kappa^2 d^2) f_{v2}$. Functions f_w and f_{v2} are defined to induce turbulence viscosity near the wall. d refers to the distance from the wall.

When we turn this standard S-A model to DES, d in equation (2) will be replaced by

$$\tilde{d} = \min\left(d, C_{\mathrm{DES}} L_{\mathrm{g}}\right). \tag{4}$$

The empirical constant C_{DES} has a value of 0.65. L_{g} is a grid length scale and defined as

$$L_{\mathrm{g}} = \max\left(\Delta x, \Delta y, \Delta z\right), \tag{5}$$

where Δx, Δy, and Δz are the local grid lengths. As a consequence, the RANS method based on the one-equation S-A model will be adopted in the region near the wall including the whole boundary layer as $\tilde{d} = d$. When the region is far from the wall, $\tilde{d} = C_{\mathrm{DES}} L_{\mathrm{g}}$, the dissipation will be determined by the local grid length. Once the dissipation term and production term reach a balance, it is found from equation (1) that $\tilde{\nu}$ is in direct proportion to $\tilde{\Omega} d^2$, that is,

$$\tilde{\nu} \propto \tilde{\Omega} {L_{\mathrm{g}}}^2. \tag{6}$$

Equation (6) has the same characteristic with the model defined by Smagorinsky [11] as a subgrid scale model used in the LES method. For a typical RANS grid with a high aspect ratio in the boundary layer, the wall-parallel grid spacing usually exceeds the boundary layer thickness, so equation (5) will ensure that the DES model is in the RANS mode for the entire boundary layer. However, in case of a dense grid in all directions, the DES limiter can activate the LES mode inside the boundary layer, where the grid is not fine enough to sustain LES requirement. Therefore, a new formulation called delayed detached eddy simulation (DDES) is presented to preserve the RANS mode throughout the boundary layer.

The length scale $\tilde{d}$ in DDES is redefined as

$$\tilde{d} = d - f_d \max\left(0, d - C_{\mathrm{DES}} L_{\mathrm{g}}\right), \tag{7}$$

where f_d is given by

$$f_d = 1 - \tan h\left([8 r_d]^3\right), \tag{8}$$

where r_d can be considered the ratio of the turbulence length scale and the wall distance. f_d is designed to be 1 in the LES region where $r_d \ll 1$ and $f_d = 0$ elsewhere. As a consequence, when flows transport from a region with a large value of eddy viscosity into a region of relatively small strain, this could cause the DDES model to switch the mode early than DES which means a transition from LES to RANS mode away from the body.

3. Test Cases

The experimental data used to validate the numerical results on a clean cavity are provided by Foster et al. [12] in 1991 at DERA, Bedford, UK. The clean cavity called the M219 cavity [13] has an aspect ratio of $L : D : W = 5 : 1 : 1$ with 10

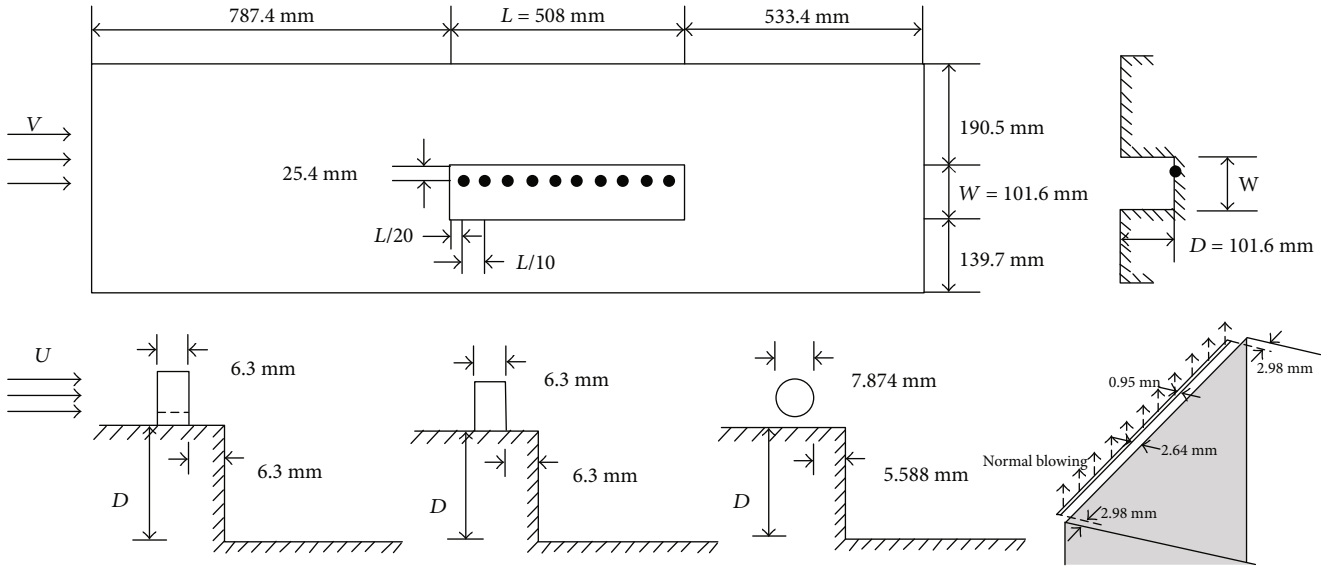

Figure 2: Geometries of cases.

equally spaced Kulite pressure sensors on the ceiling to measure the time histories of pressure with a sample frequency of 6 kHz.

The configuration of the clean cavity and three kinds of passive control devices, sawtooth spoiler, flat-top spoiler, and crossflow rod, is shown in Figure 2. According to Smith et al. [14], the height of the three devices is set to 40 percent of the boundary layer, which was around 11 mm. The blowing slot at the leading edge of the cavity is also shown in Figure 2.

The computational domain was based on the experimental rig shown in Figure 2 and extended 10D to the upper boundary. The upper boundary, inflow, and outflow were set as pressure far field boundary conditions with Ma = 0.85, static pressure $P = 62940$ Pa, static temperature $T = 270.25$ K, and eddy viscosity ratio $\mu\_t/\mu\_0 = 10$. Symmetry boundary conditions were applied on the side boundaries, and adiabatic, no-slip wall conditions were applied on the plane of the plate and all the surfaces of devices. The active blowing cases had two blowing rates, 0.0454 kg/s (0.1 lbm/s) and 0.1362 kg/s (0.3 lbm/s), respectively, on the vertical direction. The Reynolds number for all cases was 6.785×10^5.

In order to capture small-scale vortexes, the mesh around the cavity was generated meticulously with about 4.5 million cells for the clean cavity and active blowing cases and 6 million cells for the passive control cases. At the wall, the grid results in $y+<2$, which is sufficient to resolve the viscosity-affected near wall. The whole computational domain mesh for all cases is shown in Figure 3.

A Green-Gauss cell-based finite volume scheme was used with second-order implicit time integration and third-order MUSCL spatial discretization. After a steady RANS computation with the S-A model, a time step of 10^{-5} seconds with a maximum of 30 iterations per time step was selected for the DDES transient calculations. The simulation was performed for a total of 0.5 seconds with the first 0.3 seconds of data discarded to eliminate any transients leaving 0.2 seconds of computational pressure history. The simulation was performed on a cluster with 144 processors, taking 55 days for each case.

4. Results

Computational sound pressure levels (SPLs) were computed from the last 0.2 seconds of data.

$$\mathrm{SPL} = 20 \lg \left(\frac{P_{\mathrm{rms}}}{P_{\mathrm{ref}}}\right), \tag{9}$$

where $P_{\mathrm{ref}} = 2 \times 10^{-5}$ Pa is the minimum audible pressure variation. Overall sound pressure level (OASPL) was calculated as follows.

$$\mathrm{OASPL} = 10 \log_{10}\left(10^{\mathrm{SPL}_{f1}/10} + 10^{\mathrm{SPL}_{f2}/10} + \cdots + 10^{\mathrm{SPL}_{fn}/10}\right). \tag{10}$$

4.1. Passive Control. Figure 4 shows the overall SPLs from the front to the rear of the clean cavity (CC), cavity with sawtooth spoiler (STS), cavity with flat-top spoiler (FTS), and cavity with crossflow rod (CFR) configurations.

The OASPL distribution along the ceiling of the cavity in passive control cases was compared with that of the clean cavity and the experiment results in Figure 4. The overall sound pressure level of the cavity in the downstream position of the airflow is up to 167 dB, and that in the upstream position is also over 153 dB. The simulation results of the clean cavity are in good agreement with the experiment, which means that the DDES method is proper to investigate the aerodynamic noise on the cavity. It is concluded from the curves that three kinds of external devices arranged in the front edge of the cavity change the sound pressure level inside the cavity greatly. The sawtooth spoiler, flat-top spoiler, and

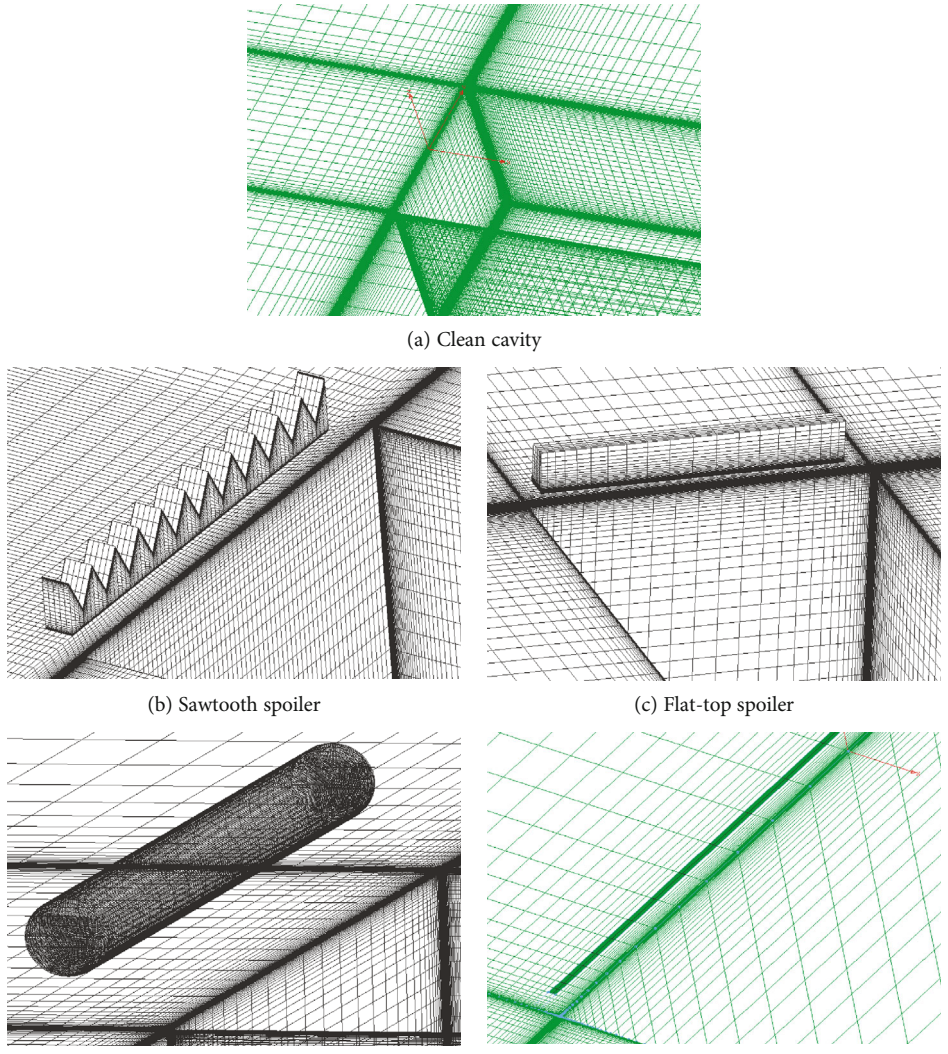

(a) Clean cavity

(b) Sawtooth spoiler

(c) Flat-top spoiler

(d) Crossflow rod

(e) Steady blowing

Figure 3: Computational mesh for all cases.

crossflow rod reduce the overall sound pressure level of the cavity by as much as 4-9 dB.

The sawtooth spoiler suppresses the sound pressure level in the front of the cavity by 4-6 dB and in the downstream from 166 dB to about 157 dB. The flat-top spoiler also has an obvious effect on noise suppression, but the general noise reduction is slightly lower than that of the sawtooth spoiler. The effect of the crossflow rod is better than that of the other two spoiler devices in the middle part of the cavity with the overall sound pressure level at $x/L = 0.45$ decreasing from 158 dB to 149 dB. In the downstream, the aeroacoustic environment became harsh, and the sawtooth spoiler performed better than the other two devices.

Figure 5 shows the sound pressure level at $x/L = 0.05$ and $x/L = 0.95$.

According to the previous research [5, 9, 15], the sound pressure level in the cavity has four distinct peaks, and the four modes are recognised as tone noise in which the second-order and third-order modes are the dominant modes. First of all, it can be seen from Figure 5 that the three passive control methods obtained by the DDES method can significantly suppress the noise level in the upstream and downstream of the cavity, especially reducing the magnitude of the second-order mode. The sawtooth spoiler and crossflow rod can effectively suppress the sound pressure level in the frequency less than 500 Hz at two positions. The flat-top spoiler reduces the magnitude of the third-order mode better than the other two devices, but the magnitude of the fourth-order mode is amplified in $x/L = 0.05$ and 0.95.

4.2. Active Control. Figure 6 shows the overall SPLs from the front to the rear of the clean cavity and cavity with steady leading edge blowing at a rate of 0.0454 kg/s and 0.1362 kg/s on normal direction.

The overall sound pressure level shown in Figure 6 is greatly suppressed at all positions, which means that the aeroacoustic environment inside the cavity is significantly improved by the steady leading edge blowing. In the 0.0454 kg/s case, the overall sound pressure level decreased by an average of 25 dB, while in the case of 0.1362 kg/s, the overall sound pressure level was reduced by an average of 30 dB. As can be seen from the figure, the curve of

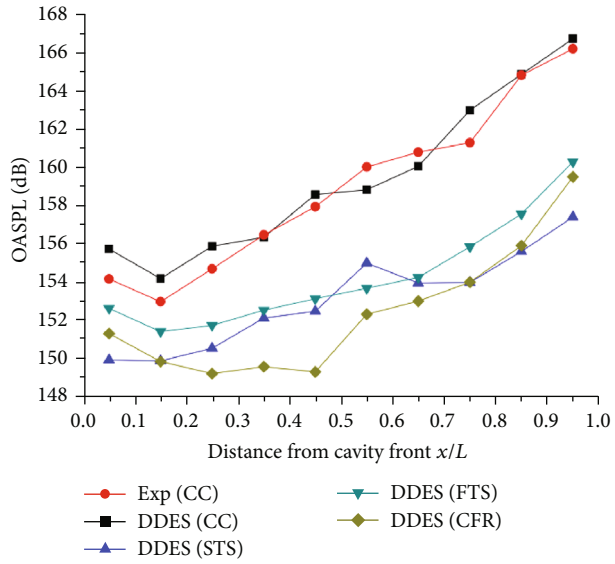

Figure 4: OASPL of passive control cases.

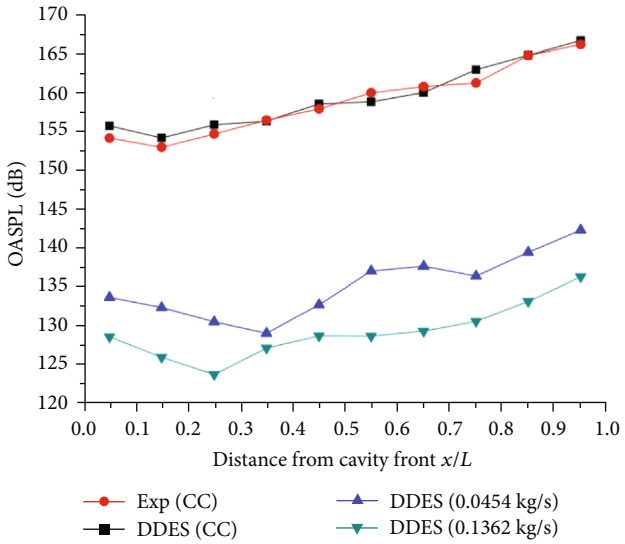

Figure 6: OASPL of active control cases.

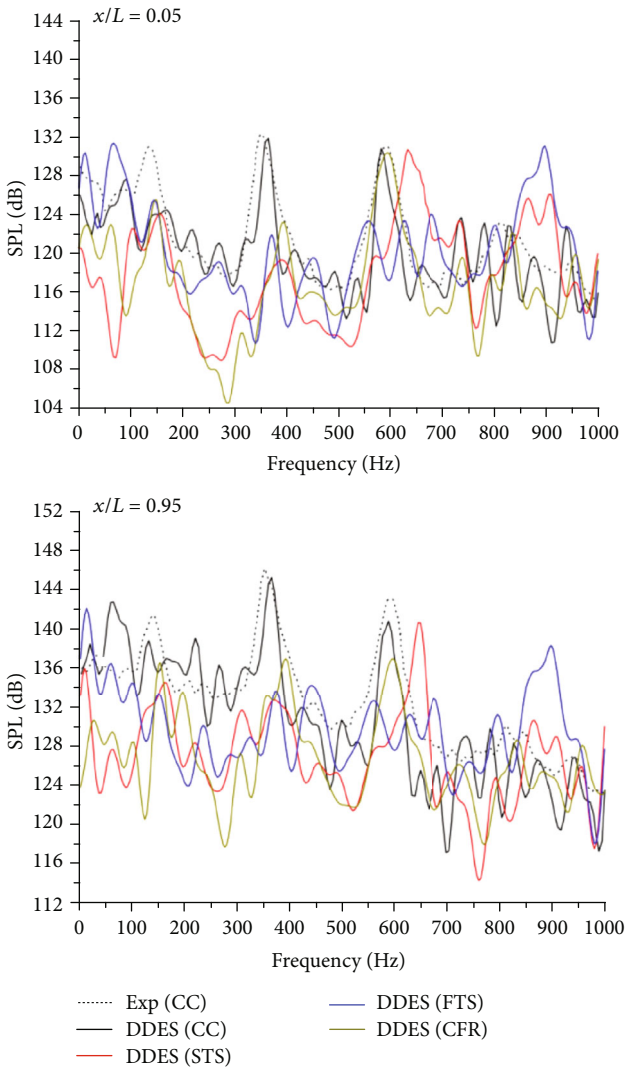

Figure 5: Sound pressure level at $x/L = 0.05$ and 0.95.

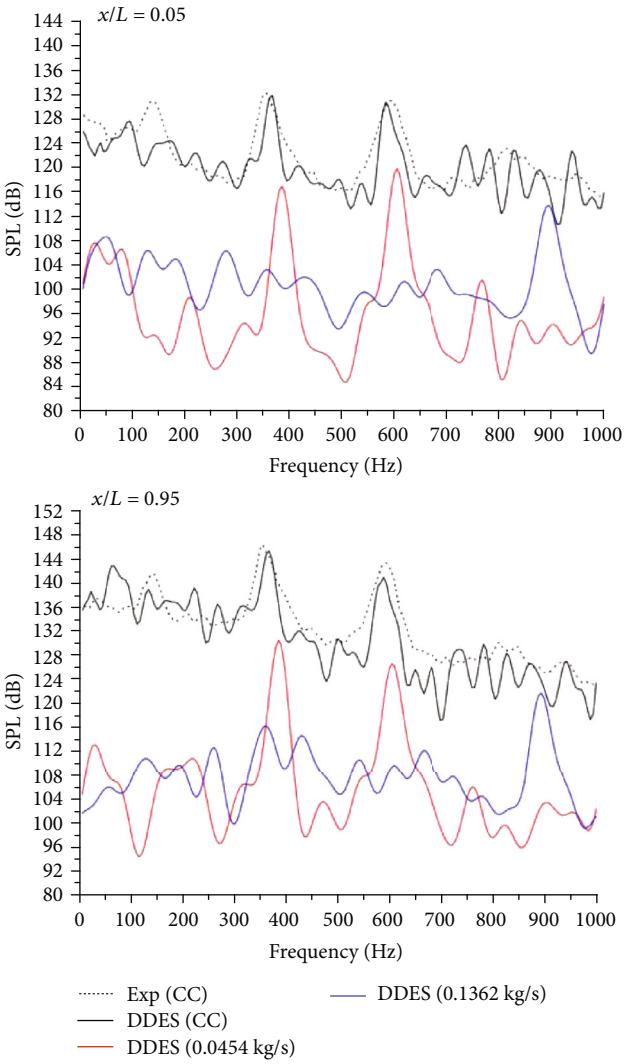

Figure 7: Sound pressure level at $x/L = 0.05$ and 0.95.

Table 1: Tone noise for all cases at $x/L = 0.95$.

Case	Mode	1st	2nd	3rd	4th
Exp. (CC)	Freq. (Hz)	142	353	592	813
	Amp. (dB)	141.6	146.3	143.4	130.2
DDES (CC)	Freq. (Hz)	67.5	366.6	589.0	738.3/783.7/827.1
	Amp. (dB)	143.0	145.5	141.0	129.1/130.0/128.4
DDES (STS)	Freq. (Hz)	164.1	371.1	647.2	867.0
	Amp. (dB)	134.7	132.8	140.7	130.6
DDES (FTS)	Freq. (Hz)	151.5	371.1	552.4	892.1
	Amp. (dB)	133.5	133.6	132.5	139.2
DDES (CFR)	Freq. (Hz)	155.1	393.3	595.3	833.4
	Amp. (dB)	136.7	137.1	137.1	128.8
DDES (0.0454 kg/s)	Freq. (Hz)	219.8	384.7	604.5	759.3
	Amp. (dB)	109.5	130.5	126.7	106.0
DDES (0.1362 kg/s)	Freq. (Hz)	129.9	359.7	669.4	894.2
	Amp. (dB)	110.8	116.3	112.2	121.7

0.0454 kg/s is W-shaped with minimum values at $x/L = 0.35$ and 0.75. However, the overall sound pressure level at the rear of the cavity is generally higher than that at the front. By the rate of 0.1362 kg/s, the overall sound pressure level distribution presents a V shape with the minimum value at $x/L = 0.25$. Compared with the clean cavity, the positon of the minimum value of OASPL along the cavity slightly moves backward. In general, the steady leading edge blowing as an active control method has a remarkable effect on the suppression of overall sound pressure level inside the cavity. Figure 7 shows the sound pressure level at $x/L = 0.05$ and $x/L = 0.95$.

It can be seen from Figure 7 that the sound pressure level for active cases still has several peaks which are tone noises. The two dominant modes in the clean cavity apparently exist in the case of 0.0454 kg/s. The dominant mode in the case of 0.1362 kg/s shifts to the high frequency band, where it used to be the fourth mode for the clean cavity. Overall, the sound pressure levels from low frequency to high frequency are all significantly suppressed at both $x/L = 0.05$ and $x/L = 0.95$ including every resonance mode. The amplitude of tone noises in the case of 0.0454 kg/s is about 13 dB smaller than that of the clean cavity. The amplitude of the dominant mode in the case of 0.1362 kg/s is reduced by 10 dB compared with that of the fourth mode in the clean cavity, and the occurrence frequency is delayed by about 100 Hz. In addition to the tone noise, the sound pressure levels at all other frequencies are effectively reduced by more than 20 dB.

4.3. Comparison of Control Methods. According to the analysis of the results, it is obvious that the aerodynamic noise environment in the downstream of the cavity is worse than that in the front. The frequency and amplitude of the resonant mode at a position of $x/L = 0.95$ are summarized in Table 1 for all passive control and active control cases.

As can be seen from Table 1, the sawtooth spoiler has a good effect on the suppression of the first two modes in the low-frequency band, with the decreasing amplitude more than 10 dB. The third mode and the fourth mode remain the same level compared with the DDES results.

Generally, the first three modes are all suppressed by the flat-top spoiler, and the amplitude of tone noise is reduced by more than 9 dB. But the fourth mode is magnified by 9 dB.

The DDES results of the crossflow rod show that the all four modes of the cavity are effectively suppressed, with the amplitude of the first two modes reduced by 7 dB and the last two modes by 3 dB. Compared with the other two passive control methods, the crossflow rod performs better in general, and the flow control effect is very stable.

The suppression effect under the condition of 0.0454 kg/s leading edge blowing is quite clear in Table 1, and the amplitude of each mode is effectively reduced. The amplitude of the second and third modes is both reduced by about 15 dB, while the amplitude of the first and fourth modes is reduced by more than 20 dB.

When the blowing rate reaches 0.1362 kg/s, the sound pressure level of the first three modes is tremendously reduced, with a drop of about 30 dB. As the fourth mode becomes the dominant mode, the amplitude reduction is not as large as that of the other three modes, but the amplitude reduction is still more than 10 dB. In general, the active control method of steady leading edge blowing can significantly suppress the sound pressure level within the cavity, especially the amplitude of the resonance mode with the reduction up to 10 dB. As the blowing rate increases from 0.0454 kg/s to 0.1362 kg/s, the sound pressure level inside the cavity is completely suppressed with the amplitude of the four modes reduced by as much as 30 dB.

In order to investigate the mechanism of the noise control methods, the instantaneous velocity profile inside the cavity for all cases at the same moment is shown in Figure 8.

It can be observed from Figure 8 that the shear layer over the cavity has an oscillation effect. The sawtooth spoiler can shift the free shear layer of the flow away from the cavity; as a result, the incoming flow directly passes over the cavity. The impact of the flow on the back edge of the cavity is

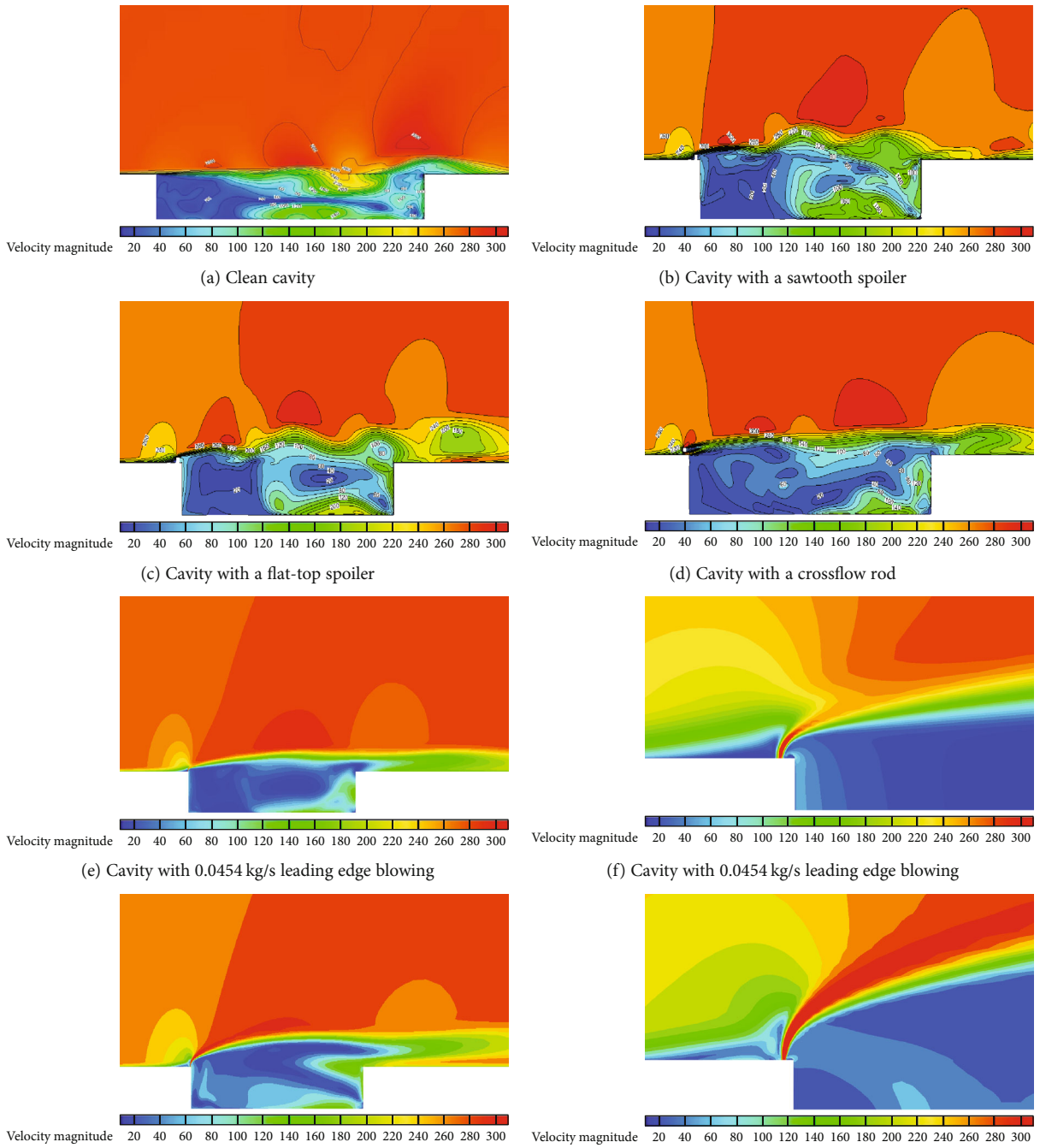

Figure 8: Profile of instantaneous velocity.

reduced, so that less energy is involved in the generation and propagation of aerodynamic noise. In addition, the sawtooth spoiler has a strong effect on splitting the flow and generates a large number of small vortexes with lower energy. The flat-top spoiler like the sawtooth spoiler can upraise the free shear layer away from the cavity, thus reducing the sound pressure level inside the cavity. The difference is that the scale of vortexes in the shear layer passing over the flat-top spoiler is bigger than that in the sawtooth spoiler. As there is a gap between the crossflow rod and the cavity wall, the shear layer is still close to the cavity like the clean cavity, but the thickness of the shear layer increases due to the crossflow rod. As a result, the thickened shear layer enters the cavity and hits the rear wall with the pressure waves generated from the wall becoming weaker. The self-sustaining oscillation effect is suppressed so as to reduce the sound pressure level inside the cavity.

The velocity profile of the active control cases shows that steady blowing perpendicular to the direction of the incoming flow has the function of pushing the free shear layer away from the cavity, which makes the incoming flow cross the cavity directly without going into it. As a consequence, a little

of flow is involved in the self-sustaining oscillation in the cavity. At the same time, the injecting flow can stabilize the shear layer and ensure the stability of the flow inside the cavity.

5. Conclusions

The DDES computations have been conducted for an open-cavity flow using the one-equation S-A model. The open cavity immersed in a free stream at a Mach number of 0.85 has an aspect ratio of 5 : 1 : 1. The passive and active flow control methods were analyzed. The passive control methods contain a leading edge sawtooth spoiler, flat-top spoiler, and crossflow rod. Active control methods include steady leading edge blowing with different jet velocities, 0.0454 kg/s and 0.1362 kg/s, respectively.

The overall sound pressure level inside the cavity is suppressed by all passive control devices; in particular, the amplitude of the second dominant mode is reduced by more than 10 dB. The sawtooth spoiler performs better at a low-frequency band, while the flat-top spoiler has an obvious effect on the first three-order modes. The crossflow rod can significantly reduce the amplitude of all the four modes, so it has great potential in engineering application on flow noise control. The active noise control method of stable leading edge blowing can significantly suppress the overall sound pressure level on each position inside the cavity with the decrement of up to 20-30 dB. In the case of 0.0454 kg/s, the magnitude of tone noise inside the cavity was reduced by as much as 15 dB. When the blowing velocity turns to 0.1362 kg/s, the sound pressure level inside the cavity is fully suppressed, and the magnitude of tone noises at all positions decreases by 30 dB.

The mechanism of cavity flow control is changing the form of the shear layer over the cavity. The steady leading edge blowing and flat-top spoiler can push the shear layer away from the cavity to avoid the high-speed flow hitting against the rear wall, and the active control methods perform much better because of the external energy injection so that minimal flow can get into the cavity. In addition to upraising the shear layer, the sawtooth spoiler can also split the incoming flow into small vortexes so as to reduce the impact energy on the rear wall. The crossflow rod can thicken the shear layer over the cavity, which slows down the self-sustained oscillation and improves the aeroacoustic environment in the cavity.

Data Availability

The clean cavity and passive control case data in the figures and table supporting the findings of this study are from previously reported studies and datasets, which have been cited. The active control case data used to support the findings of this study are currently under embargo by the funding agency. Requests for data, 12 months after publication of this article, will be considered by the corresponding authors.

Conflicts of Interest

The authors declare that they have no conflicts of interest.

Acknowledgments

This paper is supported by the National Natural Science Foundation of China (NSFC, No. 11802015). This paper is a part of a project funded by the Priority Academic Program Development of Jiangsu Higher Education Institutions (PAPD) and the Fundamental Research Funds for the Central Universities.

References

[1] M. H. Morton, C. D. Hampson, and R. A. Alexander, "Final vibration and acoustic loads development for certification of the F-22 advanced tactical fighter," in *49th AIAA/ASME/ASCE/AHS/ASC Structures, Structural Dynamics, and Materials Conference, 16th AIAA/ASME/AHS Adaptive Structures Conference,10th AIAA Non-Deterministic Approaches Conference, 9th AIAA Gossamer Spacecraft Forum, 4th AIAA Multidisciplinary Design Optimization Specialists Conference*, p. 1901, Schaumburg, IL, USA, 2008.

[2] J. Zhang, E. Morishitaf, T. Okunukil, and H. Itoh, "Experimental and computational investigation of supersonic cavity flows," in *10th AIAA/NAL-NASDA-ISAS International Space Planes and Hypersonic Systems and Technologies Conference*, p. 1755, Kyoto, Japan, 2001.

[3] K. Chung, "Characteristics of compressible rectangular cavity flows," *Journal of Aircraft*, vol. 40, no. 1, pp. 137–142, 2003.

[4] L. Shaw, "Full-scale flight evaluation of suppression concepts for flow-induced fluctuating pressures in cavities," in *20th Aerospace Sciences Meeting*, p. 329, Orlando, FL, USA, 1982.

[5] Y. Liu and M. Tong, "Comparison of passive control methods on cavity aeroacoustic using delayed detached eddy simulation," *Transaction of Nanjing University of Aeronautics and Astronautics*, vol. 32, no. 5, pp. 517–522, 2015.

[6] R. F. Schmit and G. Raman, "High and low frequency actuation comparison for a weapons bay cavity," *International Journal of Aeroacoustics*, vol. 5, no. 4, pp. 395–414, 2006.

[7] Y. Dangguo, W. Jifei, and L. Xinfu, "Investigation on suppression effect of zero-net-mass-flux jet on aerodynamic noise inside open cavities," *Acta Aeronautica et Astronautica Sinica*, vol. 32, no. 6, pp. 1007–1014, 2011.

[8] Z. Li, A. Hamed, and D. Basu, "Numerical simulation of sidewall effects on the acoustic field in transonic cavity," in *45th AIAA Aerospace Sciences Meeting and Exhibit*, p. 1456, Reno, NV, USA, January 2007.

[9] Y. Liu and M. B. Tong, "Prediction of aeroacoustic and control over a cavity by delayed detached eddy simulation," *Applied Mechanics and Materials*, vol. 598, pp. 505–509, 2014.

[10] K. D. Squires, "Detached-eddy simulation: current status and perspectives," in *Direct and Large-Eddy Simulation V*, R. Friedrich, B. J. Geurts, and O. Métais, Eds., vol. 9 of ERCOFTAC Series, Springer, Dordrecht, Netherlands, 2004.

[11] J. Smagorinsky, "General circulation experiments with the primitive equations: I. The basic experiment," *Monthly Weather Review*, vol. 91, no. 3, pp. 99–164, 1963.

[12] G. W. Foster, J. A. Ross, and R. M. Ashworth, "Weapon bay aerodynamics wind tunnel trials and CFD modeling by QinetiQ UK," in *RTO/AVT Symposium on Flow Induced Unsteady Loads and the Impact on Military Applications*, pp. 56–73, Budapest, Hungary, 2005.

[13] M. J. C. de Henshaw, "M219 cavity case-verification and validation data for computational unsteady aerodynamics," Tech. Rep. RTO-TR-26, AC/323 (AVT) TP/19, QinetiQ, Farnborough, UK, 2000.

[14] B. Smith, T. Welterlen, B. Maines, L. Shaw, M. Stanek, and J. Grove, "Weapons bay acoustic suppression from rod spoilers," in *40th AIAA Aerospace Sciences Meeting & Exhibit*, p. 662, Reno, NV, USA, 2002.

[15] Y. Liu and M. Tong, "Aeroacoustic investigation of a cavity with and without doors by delayed detached eddy simulation," *International Journal of Aeronautical and Space Sciences*, vol. 16, no. 1, pp. 19–27, 2015.